

Reflection-Based Adiabatic State Preparation

Jessica Lemieux,^{1,2,3,*} Artur Scherer,⁴ and Pooya Ronagh^{5,6,7,8}

¹*Département de Physique, Université de Sherbrooke, Sherbrooke, QC, Canada*

²*Institut Quantique, Université de Sherbrooke, Sherbrooke, QC, Canada*

³*1QB Information Technologies (1QBit), Sherbrooke, QC, Canada*

⁴*1QBit, Waterloo, ON, Canada*

⁵*1QBit, Vancouver, BC, Canada*

⁶*Institute for Quantum Computing, University of Waterloo, Waterloo, ON, Canada*

⁷*Department of Physics & Astronomy, University of Waterloo, Waterloo, ON, Canada*

⁸*Perimeter Institute for Theoretical Physics, Waterloo, ON, Canada*

We propose a circuit-model quantum algorithm for eigenpath traversal that is based on a combination of concepts from Grover’s search and adiabatic quantum computation. Our algorithm deploys a sequence of reflections determined from eigenspaces of instantaneous Hamiltonians defined along an adiabatic schedule in order to prepare a ground state of a target problem Hamiltonian. We provide numerical evidence suggesting that, for combinatorial search problems, our algorithm can find a solution faster, on average, than Grover’s search. We demonstrate our findings by applying both algorithms to solving the NP-hard MAX-2SAT problem.

I. INTRODUCTION

Grover’s search [15] is a famous quantum algorithm for unstructured search that offers a provable quadratic speed-up in comparison to exhaustive classical search. Variants of the algorithm have been studied since its invention 25 years ago [1, 9, 10, 12]. Grover’s algorithm was proven to be optimal in finding a marked element in an unstructured problem [30]. However, many industrially relevant real-world computational problems have additional structures, and exploiting them could result in potentially more-efficient heuristics that may outperform Grover’s search. Combinatorial and discrete optimization problems are examples of such structured problems. In our research, we consider the Boolean satisfiability problem as our working example. In particular, we use the NP-hard MAX-2SAT problem for our numerical studies.

We present a reflection-based adiabatic algorithm (RBA) based on a combination of concepts from Grover’s search and discrete adiabatic state preparation [2, 14, 19]. Our algorithm resembles eigenpath traversal navigated by the quantum Zeno effect [7, 8], but we replace projective measurements along the eigenpath with reflections to guide the evolution. In Sec. IID, we provide a discussion on the relationship between our research and previous work. The implementation of the RBA could follow any eigenpath traversal, such as along the instantaneous ground states of an adiabatic evolution. The algorithm’s sequence of reflections can be interpreted as slowly changing the marked state(s) when conducting a search using Grover’s algorithm.

To study the potential of the RBA, we benchmark its performance against that of Grover’s algorithm for small instances of the MAX-2SAT problem. We believe that

the RBA can also be successfully applied to solving optimization problems with non-classical objective functions. Examples of such problems include preparing the ground state of a generic Hamiltonian for fermionic systems, a problem known to be QMA-hard [17, 18, 26].

II. ALGORITHM

The RBA uses a sequence of reflections (R_1, R_2, \dots, R_L) defined by the ground states of a sequence of respective Hamiltonians. Let us denote the k -th ground state in this sequence by $|G_k\rangle$, where $k \in \{1, \dots, L\}$. The algorithm consists of the following main steps:

1. Prepare the initial state $|\text{Init}\rangle$.
2. For $k = 1, \dots, L$, apply the reflection $R_k := \mathbb{1} - 2|G_k\rangle\langle G_k|$.
3. Perform a measurement in the eigenbasis of the target problem Hamiltonian.

Depending on the type of problem, steps 1–3 may need to be repeated. We expand on the details of these steps in what follows.

A. Intermediate Hamiltonians

To define the “good” subspaces through which the reflections are applied, we introduce intermediate Hamiltonians along an adiabatic path, although our approach allows more-generic paths. For simplicity, we use a linear interpolation between the starting Hamiltonian H_0 and a problem Hamiltonian H_1 :

$$H_w := (1 - w)H_0 + wH_1. \quad (1)$$

A discretization in time corresponds to a sequence of weights (w_1, w_2, \dots, w_L) that specify the instantaneous

* Corresponding author: jessica.lemieux@1qbit.com

Hamiltonians $(H_{w_1}, H_{w_2}, \dots, H_{w_L})$. The ground states of these instantaneous Hamiltonians, respectively, characterize the corresponding good subspaces. The choice of the weights w_k could also be optimized classically by minimizing the expected energy of the resulting states, defining a hybrid quantum algorithm. These kinds of hybrid quantum–classical algorithms are often studied in the context of NISQ and variational quantum algorithms [13, 27]. The classical component of these hybrid schemes is a nontrivial optimization problem that is expected to scale poorly. For example, the barren plateau [16, 25] is the phenomenon of gradient norms decreasing exponentially fast, causing the need for exponentially many gradient estimations to be made with regard to problem size. Therefore, in Sec. III B we present the results of our study on the decay rate of the gradient norms for our hybrid scheme.

B. Reflections

The implementation of reflections requires information about the eigenstates of the intermediate Hamiltonians, which we do not have. However, this information can be coherently acquired by performing quantum phase estimation (QPE) in the basis of the respective intermediate Hamiltonian, each time a reflection is deployed. In order to do this coherently without collapsing the state, the QPE step is followed by an energy value comparison with a classical threshold E^* . This energy threshold could either be stored in an additional quantum register or be “hard-coded” in the arithmetic needed for the comparison. The result of the comparison is stored in a flag qubit. In other words, instead of measuring the energy register, which would collapse the superposition state, we obtain a flag qubit entangled with the eigenstates, such that the qubit is in the state $|1\rangle$ when the eigenstates correspond to an energy below the threshold E^* , and in the state $|0\rangle$ otherwise. Effectively, this output corresponds to marking the state around which the reflection is performed. Recall that QPE is an algorithm for estimating the phases associated with the eigenvalues of a unitary operator. In our analysis, the unitaries are given by $U_k = e^{iH_{w_k}}$, which have the same eigenstates as H_{w_k} . The phases that correspond to the eigenvalues of H_{w_k} are denoted by $E_{w_k}^j$ for every j -th eigenvalue. Thus, to ensure that QPE differentiates between all eigenstates, the Hamiltonians H_0 and H_1 must be normalized such that $0 \leq E_{w_k}^j < 2\pi$ for all k and j . Note that this approach requires us to have lower and upper bounds for the energy spectrum.

In what follows, we denote the j -th eigenstate of H_{w_k} by $|\psi_{w_k}^j\rangle$. The reflection R_k , for $k = 1, \dots, L$, can then be implemented as follows.

1. Deploy QPE with $U_k := e^{iH_{w_k}}$ and an additional register of size M used to hold the estimated energy

value:

$$\text{QPE } |0\rangle^M |\Psi\rangle = \sum_{j=0}^{2^n-1} \langle \psi_{w_k}^j | \Psi \rangle |E_{w_k}^j\rangle |\psi_{w_k}^j\rangle. \quad (2)$$

Here, $|\Psi\rangle$ is an arbitrary state and $|E_{w_k}^j\rangle$ represents the energy value corresponding to the eigenstate $|\psi_{w_k}^j\rangle$ of H_{w_k} .

2. Apply an energy value comparison with a classical threshold E^* , which requires arithmetic. Append a single-qubit ancilla initialized in the computational state $|0\rangle$. If and only if $E_{w_k}^j < E^*$, flip the ancilla. If E^* is chosen such that $E_{w_k}^0 < E^* \leq E_{w_k}^1$ (assuming the ordering¹ $E_{w_k}^0 < E_{w_k}^1 \leq E_{w_k}^2 \leq \dots$), this results in the entangled state

$$\begin{aligned} & \langle G_k | \Psi \rangle |E_{w_k}^0\rangle |G_k\rangle |1\rangle \\ & + \sum_{j=1}^{2^n-1} \langle \psi_{w_k}^j | \Psi \rangle |E_{w_k}^j\rangle |\psi_{w_k}^j\rangle |0\rangle, \end{aligned} \quad (3)$$

where $|G_k\rangle = |\psi_{w_k}^0\rangle$.

3. Apply the Pauli-Z gate to the flag ancilla, which results in a negative phase for the first term:

$$\begin{aligned} & - \langle G_k | \Psi \rangle |E_{w_k}^0\rangle |G_k\rangle |1\rangle \\ & + \sum_{j=1}^{2^n-1} \langle \psi_{w_k}^j | \Psi \rangle |E_{w_k}^j\rangle |\psi_{w_k}^j\rangle |0\rangle. \end{aligned} \quad (4)$$

4. Uncompute the registers for the energy comparison and QPE to yield the following:

$$- \langle G_k | \Psi \rangle |G_k\rangle + \sum_{j=1}^{2^n-1} \langle \psi_{w_k}^j | \Psi \rangle |\psi_{w_k}^j\rangle. \quad (5)$$

A quantum circuit diagram for these steps is shown in Fig. 1. This figure illustrates that the implementation cost of a reflection is not significantly different from that of a projective measurement. A projective measurement would terminate after QPE deployment (step 1) by measuring the register holding the energy value (cf. [8, 19]). To ensure that QPE is able to differentiate between the ground state and the first excited state, we need to estimate the phases $E_{w_k}^j$ with a precision high enough to distinguish between $E_{w_k}^0$ and $E_{w_k}^1$. In other words, the number of qubits required to hold the energy values obtained from QPE must scale as $M \in \mathcal{O}(\lceil \log_2(1/\Delta_k) \rceil)$, where $\Delta_k := E_{w_k}^1 - E_{w_k}^0$ is the k -th energy gap. As QPE scales

¹ In the event of the ground states being degenerate, the threshold is chosen to be between the ground state energy and the next energy level.

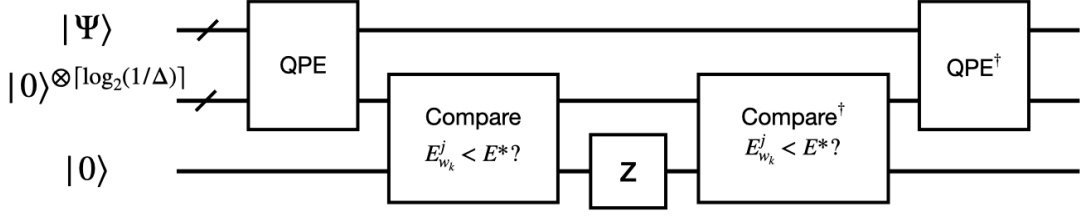


Figure 1. Quantum circuit for implementing a reflection

exponentially with respect to M , this leads to an overall scaling of $\mathcal{O}(1/\Delta)$ in terms of a lower bound on the energy gaps, $\Delta \leq \Delta_k$, for all $k = 0, \dots, L$. With respect to the reflection, adding the energy comparison scales with the number of qubits as $M \in \mathcal{O}(\lceil \log_2(1/\Delta_k) \rceil)$. The uncomputation of the ancillary registers (necessary for reversible computation) doubles the cost. Thus, a projective measurement and a reflection have roughly the same scaling in terms of query complexity, which is $\mathcal{O}(1/\Delta)$.

There are multiple alternatives for the implementation of QPE. Normally, this algorithm requires Hamiltonian simulation of the unitary $U_k = e^{iH_{w_k}}$. This is typically performed using techniques based on Lie–Trotter product formulae [4], truncated Taylor series [5], quantum signal processing [23], or qubitization [24]. Two difficulties are usually encountered when implementing QPE by digitally simulating the operator $U_k = e^{iH_{w_k}}$: the error introduced by the Hamiltonian simulation and ambiguities in the phase. Using the framework of qubitization [24], these difficulties can be eliminated by replacing U_k with the qubiterate (see Refs. [6, 19, 28]). Since the energy spectrum is changed by qubitization, using the qubiterate will affect the query complexity of the reflections. The query complexity becomes $\mathcal{O}(1/\arccos(1 - \Delta))$ instead of $\mathcal{O}(1/\Delta)$ [19, 24]. There are also techniques that incorporate the linear combination of unitaries or oblivious amplitude amplification [11]. However, in view of the actual purpose of our work, we do not include these additional improvements. For simplicity, our analysis is based on the original approach of implementing QPE by simulating the unitary U_k .

C. Connection to Grover’s Search Algorithm

Grover’s search [15], and the related amplitude amplification algorithm [10], use two reflections: one through the subspace spanned by the superposition state in the “good” subspace, $|\text{Succ}\rangle$, and another one through the subspace spanned by the initial state, $|\text{Init}\rangle$:

$$R_1^G = \mathbb{1} - 2|\text{Succ}\rangle\langle\text{Succ}| = e^{i\pi|\text{Succ}\rangle\langle\text{Succ}|}, \quad (6)$$

$$R_2^G = \mathbb{1} - 2|\text{Init}\rangle\langle\text{Init}| = e^{i\pi|\text{Init}\rangle\langle\text{Init}|}. \quad (7)$$

The algorithm repeatedly applies R_1 followed by R_2 , whose combined effect is called the Grover iteration. The key uncertainty is in figuring out when to stop

to achieve the highest probability of success. If $|\langle\text{Succ}|\text{Init}\rangle| = \sin(\theta/2)$, the optimal number of Grover iterations is $n_{\text{it}}^{\text{opt}} = \lceil \frac{\pi}{2\theta} - \frac{1}{2} \rceil$, in which case the algorithm outputs a solution state with a success probability equal to $\sin^2[(n_{\text{it}}^{\text{opt}} + 1/2)\theta]$. However, we generally do not know the overlap $|\langle\text{Succ}|\text{Init}\rangle|$. Since the probability of success is periodic in n_{it} in this scheme, exceeding $n_{\text{it}}^{\text{opt}}$ results in its decrease. As for discrete adiabatic state preparation [7], in our scheme, increasing the number of intermediate steps will most likely increase the probability of success.

On the other hand, Grover’s algorithm can also be viewed as a special case of the RBA, where the weights w_k alternate between 0 and 1. Alternatively, imagine a perfectly defined reflection that maps the initial state to the desired target state in a single step. It can be shown that the gap of the intermediate Hamiltonian corresponding to such a reflection would be exactly $\sin(\theta/2)$ (similar to the proof made by Roland and Cerf [29]). Thus, implementing this reflection using the steps described in the previous section would lead to the same scaling, because the gap determines the precision needed for QPE. Moreover, implementing a Trotter–Suzuki decomposition of this reflection, with R_1^G and R_2^G as the composing operators, would require a number of iterations that also scales with $1/\sin(\theta/2)$. Hence, we get the same scaling as for Grover’s algorithm.

D. Connection to Eigenpath Traversal

The RBA performs a sequence of reflections to guide the evolution of a quantum state. This sequence of reflections can be found by a discretization of an adiabatic path, where the reflections are applied through the subspaces spanned by the ground states of the instantaneous Hamiltonians chosen. Previous studies have shown that the traversal of an eigenpath can be accomplished by a scheme resembling the quantum Zeno effect [7, 8, 19], preparing the target states with high fidelity by performing a sequence of projective measurements. Normally, the quantum Zeno effect involves frequently performing projective measurements that are all in the same basis, effecting a suppression of the system’s own dynamics and “localizing” its quantum state in one of the eigensubspaces of the measured observable. In the context of an adiabatic scheme, however, the measurement basis is

continually changed during the computation: in order to drag the system along an adiabatic evolution, the system state is projected onto the ground state of the instantaneous Hamiltonians of the corresponding adiabatic schedule. In the unlikely event of failure, the ground state can be recovered using a rewind procedure [19].

It should be noted that the algorithm by Boixo et al. [8] also uses reflections along the eigenpath (defined as a sequence of eigenstates $|\psi_s\rangle$, for $0 \leq s \leq 1$, of unitary operators U_s or Hamiltonians H_s). However, in that scheme, each instantaneous reflection is controlled by an ancilla that is used to flag the desired eigenstate $|G_k\rangle$ in that step. This flag qubit is subsequently measured, which is, in effect, the implementation of a binary projective measurement $\{|G_k\rangle\langle G_k|, \mathbb{1} - |G_k\rangle\langle G_k|\}$. In the event of failure, another reflection is used to introduce a significant overlap with $|G_k\rangle$. This is akin to the effect of performing a rewind procedure used by Lemieux et al. [19]. These operations are repeated until the flag qubit signals the $|G_k\rangle$ has been successfully prepared. Hence, although using reflections, the overall progression of the algorithm [8] results in a quantum Zeno effect-like eigenpath traversal. In contrast, the RBA does not rely on intermediate projective measurements. Instead, it deploys consecutive reflections around the instantaneous eigenstates to traverse the eigenpath without forcing the evolving system state to “localize” in the instantaneous eigensubspace at each step along the schedule.

In what follows, we demonstrate that a reflection around an intermediate state gives a better probability of success than a binary projective measurement defined by the same state.

Let us denote the initial state and the final state by $|I\rangle$ and $|F\rangle$, respectively. Beginning with $|I\rangle$, we aim to reach $|F\rangle$ with as high a probability as possible. Furthermore, let us introduce a sequence of binary projective measurements, $\{P_k, \bar{P}_k\}$, where $P_k := |k\rangle\langle k|$ and $\bar{P}_k := \mathbb{1} - P_k$, as well as a sequence of independent corresponding reflections, $R_k = \mathbb{1} - 2|k\rangle\langle k|$, for $k \in \{1, \dots, L\}$. Using the triangle inequality, given

$$\delta P := |\langle F|P_k|I\rangle| - |\langle F|I\rangle| \geq 0, \quad (8)$$

we have

$$\delta R := |\langle F|R_k|I\rangle| - |\langle F|I\rangle| \geq 2\delta P. \quad (9)$$

In other words, if an intermediate projective measurement improves the overlap between the initial and the final states, then the corresponding reflection will cause an even greater overlap. This also means that we can increase the probability of success by adding a reflection whenever adding the corresponding projective measurement is advantageous. Similarly, the use of a telescoping sum implies that

$$|\langle F|\prod_{k=1}^L R_k|I\rangle| - |\langle F|I\rangle| = \sum_{k=1}^L \delta R_k \geq 2 \sum_{k=1}^L \delta P_k, \quad (10)$$

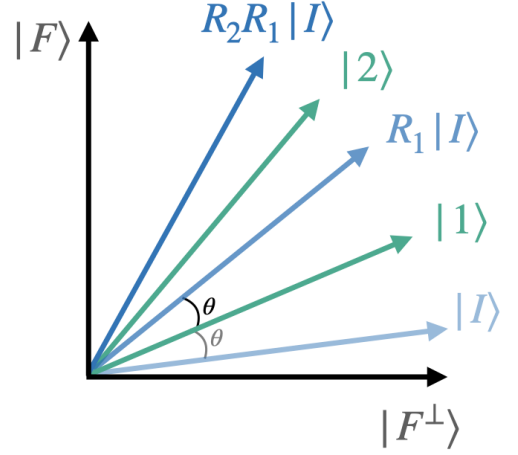


Figure 2. Visualization of the reflection-based preparation of the target state when adding reflections increases the overlap with the target state, as $|\langle F|P_2 R_1|I\rangle| > |\langle F|R_1|I\rangle|$

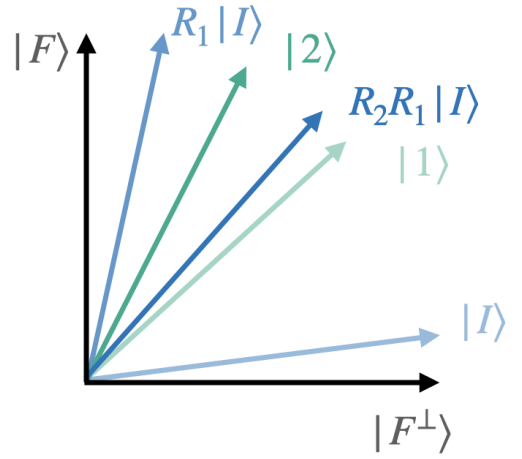


Figure 3. Visualization of the reflection-based preparation of the target state when adding a second reflection decreases the overlap with the target state, as $|\langle F|P_2 R_1|I\rangle| < |\langle F|R_1|I\rangle|$

where

$$\delta R_k := |\langle F|\prod_{j=1}^k R_j|I\rangle| - |\langle F|\prod_{j=1}^{k-1} R_j|I\rangle| \quad (11)$$

and

$$\delta P_k := |\langle F|P_k \prod_{j=1}^{k-1} R_j|I\rangle| - |\langle F|\prod_{j=1}^{k-1} R_j|I\rangle|. \quad (12)$$

We illustrate these concepts in Fig. 2 and in Fig. 3. Figure 2 shows when the condition needed to improve the probability of success is satisfied. Figure 3 illustrates the case when, even if making two projective measurements would increase the probability of success as compared to just one, the condition for increasing the probability

of success by adding a second reflection is not satisfied. Note that in the latter case, performing one reflection is actually better than making two projective measurements to increase the overlap with the target state. For details on the assumption that intermediate projective measurements will result in an increase in the overlap, see the work of Aharonov and Ta-Shma [3] and Boixo et al. [7].

III. PERFORMANCE ANALYSIS OF THE RBA

To study the RBA, we compare its performance to Grover's search. We use the NP-hard MAX-2SAT problem as the reference problem.

A. Application to the MAX-2SAT Problem

In its conjunctive normal form, each MAX-2SAT problem instance can be expressed as the Boolean formula

$$\bigwedge_{c \in \mathcal{C}} (\ell_{c_1} \vee \ell_{c_2}), \quad (13)$$

where \mathcal{C} denotes the set of all clauses composing the formula. Here,

$$\ell_{c_1}, \ell_{c_2} \in \{v_0, \neg v_0, \dots, v_{n-1}, \neg v_{n-1}\} \quad (14)$$

are a pair of distinct literals specifying a clause $c \in \mathcal{C}$, and $v_k \in \{\text{TRUE}, \text{FALSE}\}$, for $k = 0, 1, \dots, n-1$, are n Boolean variables. Notice that c_1 and c_2 serve as labels for the two literals making up the clause c . For instance, for the clause $c = (\neg v_i \vee v_j)$, $c_1 = i$ and $c_2 = j$. The problem consists in the task of determining the maximum number of clauses $c \in \mathcal{C}$ that can be simultaneously satisfied by an assignment to the Boolean variables.

The MAX-2SAT problem can be recast as the problem of finding the ground state of the 2-local Hamiltonian

$$H_c := \sum_{c \in \mathcal{C}} \left((-1)^{\nu(\ell_{c_1})} (-1)^{\nu(\ell_{c_2})} Z_{c_1} Z_{c_2} + (-1)^{\nu(\ell_{c_1})} Z_{c_1} + (-1)^{\nu(\ell_{c_2})} Z_{c_2} \right), \quad (15)$$

where Z_k represents the Pauli operator pertaining to variable v_k , $\nu(\ell) = 0$ if the literal ℓ is not negated, and $\nu(\ell) = 1$ if it is. The mapping of the MAX-2SAT problem to the Hamiltonian is such that the eigenvalues $+1$ and -1 of the Pauli- Z_k operator correspond to the Boolean values FALSE and TRUE of the variable v_k , respectively. The energy spectrum of this Hamiltonian is such that, every time a clause is not satisfied for a given variable assignment, there is a corresponding energy penalty of $+3$, and if a clause is satisfied, its energy contribution is -1 . Therefore, the ground states of this Hamiltonian correspond to the variable assignments that

satisfy the maximum number of clauses. By shifting the energy spectrum by $|\mathcal{C}|$, the ground state energy would be equal to zero if the problem is satisfiable, and higher if it is not. This way, at any iteration, if the outcome of measuring the energy is zero, it is certain that the problem is satisfiable. Also, note that the entire spectrum is upper bounded by $4|\mathcal{C}|$.

In our analysis, the initial state is chosen to be the uniform superposition

$$|+\rangle^{\otimes n} := \text{HAD}^{\otimes n} |0\rangle^{\otimes n} = \frac{1}{\sqrt{2^n}} \sum_{k=0}^{2^n-1} |k\rangle, \quad (16)$$

which can be easily generated by applying a Hadamard gate HAD to each qubit. This state is the ground state of the transverse field Hamiltonian

$$H_{\text{trans}} := - \sum_{k=0}^{n-1} X_k, \quad (17)$$

which is commonly chosen as the initial Hamiltonian of the adiabatic schedule, where X_k is the Pauli- X operator corresponding to v_k .

B. Numerical Study

Our numerical benchmark includes simulations of the success probability of the RBA and a cost analysis in comparison to Grover's search in solving small MAX-2SAT problem instances. Our results pertain to classically optimized sets of reflection points and the ideal choice of scaling parameters for H_0 and H_1 . Note that, in practice, to optimize reflection points along the path, we would need to sample the final energy and use a classical optimizer to find a (sub-)optimal schedule for the reflections.

Our numerical simulations use the following steps.

1. Perform the ideal normalization as follows:

$$\begin{aligned} H_0 &:= 2\pi(H_{\text{trans}} - E_{\text{trans}}^0 \mathbb{1}) / (E_{\text{trans}}^{2^n-1} - E_{\text{trans}}^0), \\ H_1 &:= 2\pi(H_c - E_c^0 \mathbb{1}) / (E_c^{2^n-1} - E_c^0), \end{aligned} \quad (18)$$

where E_{trans}^j and E_c^j for $j = 0, \dots, (2^n - 1)$ are the eigenvalues of energies of the Hamiltonian H_{trans} and H_c , respectively.

2. Set the total number of reflection points $L = 1$.
3. Use the Nelder-Mead optimization protocol to find a set $\{w_1, \dots, w_L\}$ of reflection points (by minimizing the probability of failure), assuming energy thresholds between $E_{w_k}^0$ and $E_{w_k}^1$ for all $k = 1, \dots, L$, and compute the time to solution (TTS).
4. Repeat the previous step by performing $L = 2, 3, 4, \dots$ reflections until a minimum TTS is observed.

In practice, we do not have access to $E_{w_k}^0$ and $E_{w_k}^1$ in step 3. However, we may use the known values of both E_0^0 and E_0^1 , and an upper bound for E_1^0 determined using other techniques (e.g., polynomial-time approximation schemes [21] or local heuristic search methods [22]), to construct a concave threshold function with respect to w and tune the concavity of the function to estimate tight upper bounds for $E_{w_k}^0$ for all reflection points w_k . We also note that the normalization in step 1 is considered “ideal” since we do not have access to E_1^0 or $E_1^{2^n-1}$. However, we can use $4|C|$, or another heuristically found bound, as an upper bound for $(E_1^{2^n-1} - E_1^0)$.

For small problem instances with the number of variables $n \in \{5, \dots, 13\}$, we compute the probability of success p_s (i.e., the modulus squared of the overlap between the final computational state and the target state), given the above choices of threshold, reflection points, and normalization. The TTS is then given by

$$\text{TTS}_{\text{RBA}} = \frac{\log \epsilon}{\log(1 - p_s)} \sum_{k=0}^L \frac{2r}{\Delta_k}, \quad (19)$$

where $\Delta_k = E_{w_k}^1 - E_{w_k}^0$ is the normalized instantaneous energy gap, $r := |C|/n$, and ϵ is the overall allowable probability of failure. In our simulations, we set $\epsilon = 0.1$.

In Eq. (19), the cost of each trial of the algorithm is $\sum_{k=0}^L \frac{2r}{\Delta_k}$, as QPE requires a number of queries to Hamiltonian simulation unitaries that scales with the inverse of the precision needed to distinguish between the energies of the first excited state and the ground state. Moreover, each unitary has a gate depth that scales with the ratio r .

The TTS for Grover’s algorithm is given by

$$\begin{aligned} \text{TTS}_{\text{Grover}} &= \frac{\log \epsilon}{\log(1 - p_s)} \sum_{k=1}^{n_{it}} \frac{2r}{\Delta_T} \\ &= \frac{\log \epsilon}{\log(1 - p_s)} \frac{2n_{it}r}{\Delta_T}, \end{aligned} \quad (20)$$

where $\Delta_T = 2\pi(E_c^1 - E_c^0)/(E_c^{2^n-1} - E_c^0)$ is the normalized gap pertaining to the target Hamiltonian. Note that we ignore the additional cost of R_1^G .

We generate 20 distinct random instances for each problem size and each $r \in \{4, 6, 8\}$ (with the exception of the combination $n = 5$ and $r = 8$, in which case there is only one possible instance), and compute the corresponding TTS values. We plot the results we obtain for the RBA against those we obtain for Grover’s search in Fig. 4 and in Fig. 5, where we can see a trend indicating a speed-up relative to Grover’s search. The TTS depends on both n and r . The impact of both of these parameters is shown in colour, with the colour bars indicating the number of variables in Fig. 4 and the ratio in Fig. 5.

These figures illustrate that, for small problem instances, Grover’s algorithm performs better, but, as the problem becomes harder, the RBA tends to outperform



Figure 4. Improvement in TTS for the RBA compared to Grover’s search. The colours indicate the number of variables used for each problem instance.

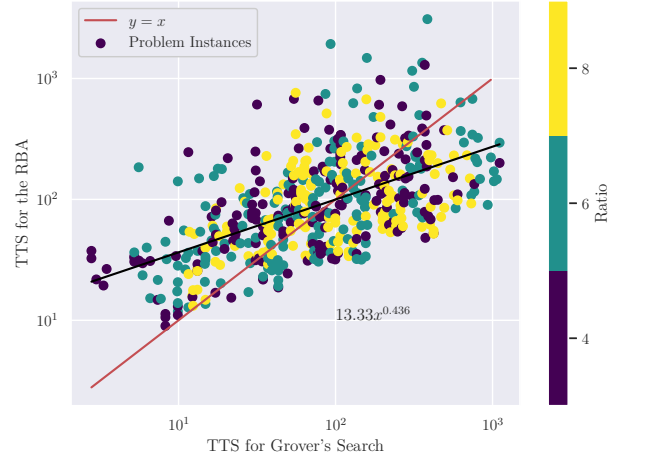


Figure 5. Improvement in TTS for the RBA compared to Grover’s search. The colours indicate the ratio used for each problem instance.

Grover’s algorithm. The reason is that the number of iterations required for our algorithm to reach a high probability of success grows more slowly with the system size than in Grover’s search, as shown in Fig. 6, but each reflection has a higher cost (due to there being a smaller gap for the instantaneous Hamiltonian in comparison to H_0 and H_1).

Figure 6 shows the median values of the number of iterations required for both algorithms to reach a target probability of failure below 0.2. As expected, for Grover’s algorithm, we observe an exponential dependence of the number of iterations on the number of variables. For the RBA, the nature of this relationship is not readily apparent. As the number of iterations is discrete and we only include simulations for problem instances with

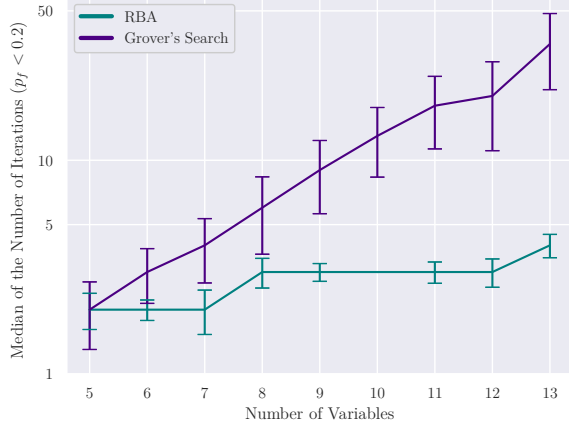


Figure 6. Median of the number of iterations versus the number variables for the RBA and Grover's search that is needed to obtain a probability of failure below a value of 0.2

up to 13 variables, it is hard to extract a clear trend. However, we observe a significant decrease in the number of iterations as compared to Grover's search.

The TTS scaling of the RBA could potentially be reduced by using the method of qubitization [6, 19, 24, 28]. Indeed, qubitization would change the overlap between successive states as well as the gap from Δ to $\arccos(1 - \frac{\Delta}{2\pi})$, which has a greater impact for smaller gap values [19]. This could potentially result in a further improvement of the RBA over Grover's search.

For a hybrid approach, in which we optimize the choice of each w_k using a classical optimizer, we study the phenomenon of the barren plateau. To do so, we compute the variance $\text{var}\left(\frac{\partial E}{\partial w_i}\right)$ when $L = 2$. We consider the same problem instances as earlier. To sample the variation in energy based on the positions of the reflections, we take 5000 random points uniformly distributed from within the intervals $(\frac{1}{6}, \frac{1}{2})$ and $(\frac{1}{2}, \frac{5}{6})$. In Fig. 7, we observe an exponential decay with a rate of 0.08 for the median values of gradient variances. This is in contrast to the rate of 0.685 obtained for the random parameterized quantum circuits studied by McClean et al. [25]. The error bars indicate the standard deviation.

Figure 8 shows the TTS ratio of the non-optimized RBA (i.e., using equidistant reflection points between 0 and 1) over one that optimizes the reflection points versus the number of reflections (i.e., the advantage offered by the classical optimizer). We observe that not performing the optimization adds, on average, a linear factor with the number of reflections. Notice that, in some cases, the non-optimized version has a smaller TTS. This is because we minimize the probability of failure and not the TTS. Indeed, for some cases, the smaller probabilities of success exist alongside larger gaps, which can result in a smaller TTS. Figure 9 shows the TTS for the non-optimized RBA compared to the TTS for Grover's search.

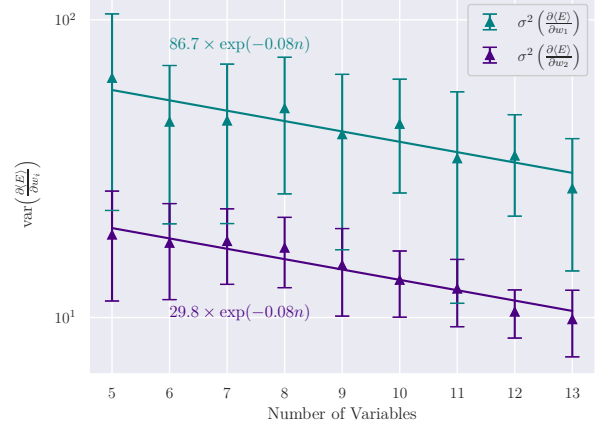


Figure 7. Variance of the partial derivative of the expected energy versus the number of variables for the RBA, demonstrating an exponential decay associated with the existence of a barren plateau for a schedule with two reflections

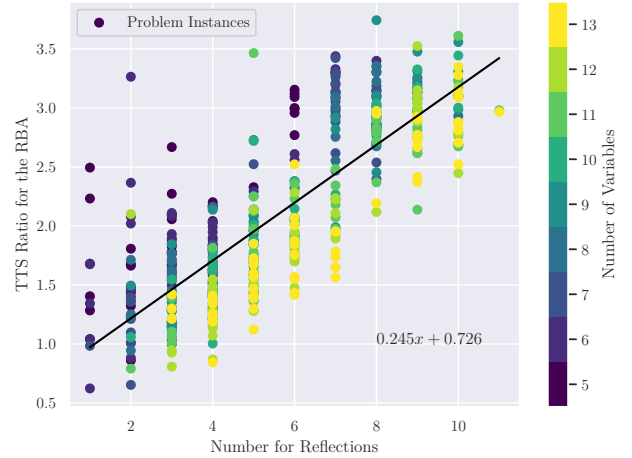


Figure 8. Time-to-solution ratio of the non-optimized RBA over one that is optimized versus the number of reflections. The non-optimized RBA uses a schedule with equidistant reflection points. The optimized RBA uses a schedule that minimizes the probability of failure. A decrease in the TTS resulting from optimizing the positions of the reflections can be seen. The colours indicate the number of variables used for each problem instance.

We observe that, even with a schedule with equidistant reflection points, the RBA offers a speed-up over Grover's search. Figure 9 is equivalent to Fig. 4, except that it does not include the optimization of the reflection points.

Finally, we empirically study the impact of having an energy threshold between $E_{w_k}^1$ and $E_{w_k}^2$ and observe that it does not result in a significant increase in the TTS. In fact, in some cases, it results in a decrease in the TTS, especially for instances that exhibit a closing energy gap toward the end of the adiabatic path. This is due to

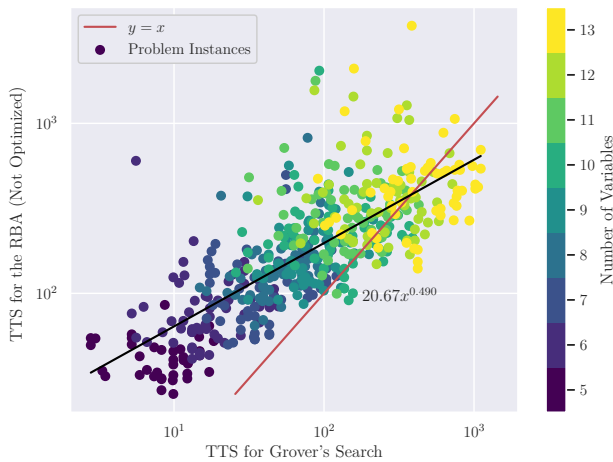


Figure 9. Time to solution for the non-optimized RBA versus the TTS for Grover’s search. Optimization of the reflection points is not performed; the figure is otherwise equivalent to Fig. 4. The non-optimized RBA uses a schedule with equidistant reflection points. The colours indicate the number of variables used for each problem instance.

there being a reduced-precision requirement needed to implement QPE. Indeed, in this case, the precision requirement scales inversely with $(E_{w_k}^2 - E_{w_k}^0)$ instead of with $(E_{w_k}^1 - E_{w_k}^0)$. Thus, we expect that the RBA is not significantly sensitive to optimal choices of energy thresholds.

IV. CONCLUSION

We have presented a new circuit-model quantum algorithm for preparing the ground state of a target problem Hamiltonian. The reflection-based adiabatic algorithm (RBA) is based on a combination of concepts from Grover’s search and adiabatic quantum computation. We have shown that the resource requirements for the RBA to reach the target state with a high probability of success scale favourably compared to Grover’s search in solving MAX-2SAT problem instances. We used the time-to-solution metric (TTS), that is, the time needed to find a solution for a particular problem instance with high confidence (e.g., a rate of 90%). Although our algorithm has a higher implementation cost per reflection, as the probability of success increases faster with the number of reflections than it does in Grover’s search, the TTS scales better.

The complexity analysis made by Boixo et al. [8] suggests that path traversal algorithms could outperform Grover’s algorithm in solving search and optimization problems. In the present work, we have provided numerical evidence supporting this claim. Although the RBA does not employ projective measurements but instead uses reflections to traverse the eigenpath, the inequali-

ties from Sec. IID suggest that its query complexity is not worse than given by Boixo et al. [8].

Previous work on discrete adiabatic state preparation using continual instantaneous projective measurements [19] incorporated techniques such as qubitization [24] and a rewind procedure. We expect that qubitization would also reduce the implementation cost of the reflections in the RBA. However, a rewind procedure is not helpful in a unitary scheme (i.e., without projective measurements); thus, we have not employed such a procedure in our implementation, which benefits from full quantum parallelism. Indeed, it is not only the ground states along an adiabatic path that contribute to the probability amplitude of obtaining the desired target state, but so do the excited states. The contribution of the excited states becomes especially important in schemes where the gap closes toward the end of the adiabatic schedule, which is the case for degenerate instances of MAX- k SAT problems. Moreover, in real-world experiments, the measurements required in measurement-based adiabatic schemes are generally slower and much more prone to suffering from errors than are unitary quantum gates. In light of our findings, we also believe that the heuristic use of the walk operator by Lemieux et al. [20] works well without employing phase randomization [7], because the walk operator consists of reflections.

In looking toward potential implementations of a hybrid RBA scheme supplemented by a classical optimization loop, we have investigated the barren plateau phenomenon. Our simulations indicate that there is a small exponential decay associated with the existence of a barren plateau, with a rate of 0.08. However, the decrease in the TTS resulting from optimizing the positions of reflections along an adiabatic path scales linearly with the number of reflections. Since the number of reflections employed in the RBA scales more slowly than that in Grover’s search, we expect that, even without optimization, the RBA algorithm will provide a greater speed-up, on average, than Grover’s search.

ACKNOWLEDGEMENT

The authors thank our editor, Marko Bucyk, for his careful review and editing this manuscript, Simon Verret and Gili Rosenberg for helpful discussions. P. R. additionally acknowledges the financial support of Mike and Ophelia Lazaridis, and Innovation, Science and Economic Development Canada.

- [1] Scott Aaronson and Patrick Rall. Quantum Approximate Counting, Simplified. In *Symposium on Simplicity in Algorithms*, pages 24–32. SIAM, 2020. doi:10.1137/1.9781611976014.5.
- [2] Dorit Aharonov and Amnon Ta-Shma. Adiabatic quantum state generation and statistical zero knowledge. In *STOC '03: Proceedings of the thirty-fifth annual ACM symposium on Theory of Computing*, pages 20–29, 2003. doi:10.1145/780542.780546.
- [3] Dorit Aharonov and Amnon Ta-Shma. Adiabatic Quantum State Generation. *SIAM Journal on Computing*, 37(1):47–82, 2007. doi:10.1137/060648829.
- [4] Dominic W. Berry, Graeme Ahokas, Richard Cleve, and Barry C. Sanders. Efficient Quantum Algorithms for Simulating Sparse Hamiltonians. *Communications in Mathematical Physics*, 270:359–371, 2007. doi:10.1007/s00220-006-0150-x.
- [5] Dominic W. Berry, Andrew M. Childs, Richard Cleve, Robin Kothari, and Rolando D. Somma. Simulating Hamiltonian Dynamics with a Truncated Taylor Series. *Physical Review Letters*, 114:090502, Mar 2015. URL: <https://journals.aps.org/prl/abstract/10.1103/PhysRevLett.114.090502>, doi:10.1103/PhysRevLett.114.090502.
- [6] Dominic W. Berry, Mária Kieferová, Artur Scherer, Yuval R. Sanders, Guang Hao Low, Nathan Wiebe, Craig Gidney, and Ryan Babbush. Improved techniques for preparing eigenstates of fermionic Hamiltonians. *npj Quantum Information*, 4:1(22):10501, 2018. doi:10.1038/s41534-018-0071-5.
- [7] Sergio Boixo, Emanuel Knill, and Rolando D. Somma. Eigenpath traversal by phase randomization. *Quantum Information and Computation*, 9(9&10):833–855, 2009. doi:10.26421/QIC9.9-10-7.
- [8] Sergio Boixo, Emanuel Knill, and Rolando D. Somma. Fast quantum algorithms for traversing paths of eigenstates. *arXiv:1005.3034*, 2010. URL: <https://arxiv.org/abs/1005.3034>.
- [9] Michel Boyer, Gilles Brassard, Peter Høyer, and Alain Tapp. Tight Bounds on Quantum Searching. *Fortschritte der Physik: Progress of Physics*, 46(4-5):493–505, 1998. doi:10.1002/(SICI)1521-3978(199806)46:4/5<493::AID-PROP493>3.0.CO;2-P.
- [10] Gilles Brassard, Peter Høyer, Michele Mosca, and Alain Tapp. Quantum Amplitude Amplification and Estimation. *Contemporary Mathematics*, 305:53–74, 2002. URL: <http://dx.doi.org/10.1090/conm/305>, doi:10.1090/conm/305/05215.
- [11] Anirban Narayan Chowdhury, Yigit Subasi, and Rolando D. Somma. Improved implementation of reflection operators. *arXiv:1803.02466*, 2018. URL: <https://arxiv.org/abs/1803.02466>.
- [12] Christoph Dürr and Peter Høyer. A Quantum Algorithm for Finding the Minimum. *arXiv:quant-ph/9607014*, 1996. URL: <https://arxiv.org/abs/quant-ph/9607014>.
- [13] Edward Farhi, Jeffrey Goldstone, and Sam Gutmann. A Quantum Approximate Optimization Algorithm. *arXiv:1411.4028*, 2014. URL: <https://arxiv.org/abs/1411.4028>.
- [14] Edward Farhi, Jeffrey Goldstone, Sam Gutmann, Joshua Lapan, Andrew Lundgren, and Daniel Preda. A Quantum Adiabatic Evolution Algorithm Applied to Random Instances of an NP-Complete Problem. *Science*, 292(5516):472–475, 2001. doi:10.1126/science.1057726.
- [15] Lov K. Grover. A fast quantum mechanical algorithm for database search. In *STOC '96: Proceedings of the twenty-eighth annual ACM symposium on Theory of Computing*, pages 212–219, 1996. doi:10.1145/237814.237866.
- [16] Zoë Holmes, Kunal Sharma, M. Cerezo, and Patrick J. Coles. Connecting ansatz expressibility to gradient magnitudes and barren plateaus. *arXiv:2101.02138*, 2021. URL: <https://arxiv.org/abs/2101.02138>.
- [17] Julia Kempe, Alexei Kitaev, and Oded Regev. The Complexity of the Local Hamiltonian Problem. *Siam Journal of Computing*, 35(5):1070–1097, 2006. doi:10.1007/978-3-540-30538-5_31.
- [18] Alexei Yu Kitaev, Alexander Shen, and Mikhail N. Vayli. *Classical and Quantum Computation*, volume 47. American Mathematical Society, 2002. URL: <http://dx.doi.org/10.1090/gsm/047>, doi:10.1090/gsm/047.
- [19] Jessica Lemieux, Guillaume Duclos-Cianci, David Sénéchal, and David Poulin. Resource estimate for quantum many-body ground-state preparation on a quantum computer. *Physical Review A*, 103:052408, May 2021. URL: <https://link.aps.org/doi/10.1103/PhysRevA.103.052408>, doi:10.1103/PhysRevA.103.052408.
- [20] Jessica Lemieux, Bettina Heim, David Poulin, Krysta Svore, and Matthias Troyer. Efficient quantum walk circuits for Metropolis–Hastings algorithm. *Quantum*, 4:287, 2020. doi:10.22331/q-2020-06-29-287.
- [21] Michael Lewin, Dror Livnat, and Uri Zwick. Improved rounding techniques for the MAX 2-SAT and MAX DI-CUT problems. In *International Conference on Integer Programming and Combinatorial Optimization*, pages 67–82. Springer, 2002. doi:10.1007/3-540-47867-1_6.
- [22] Chu-Min Li and Felip Manyà. Theory and Applications of Satisfiability Testing–SAT 2021. 2009. doi:10.1007/978-3-030-80223-3.
- [23] Guang Hao Low and Isaac L. Chuang. Optimal Hamiltonian Simulation by Quantum Signal Processing. *Physical Review Letters*, 118:010501, Jan 2017. URL: <https://link.aps.org/doi/10.1103/PhysRevLett.118.010501>, doi:10.1103/PhysRevLett.118.010501.
- [24] Guang Hao Low and Isaac L. Chuang. Hamiltonian Simulation by Qubitization. *Quantum*, 3:163, 2019. doi:10.22331/q-2019-07-12-163.
- [25] Jarrod R. McClean, Sergio Boixo, Vadim N. Smelyanskiy, Ryan Babbush, and Hartmut Neven. Barren plateaus in quantum neural network training landscapes. *Nature communications*, 9(1):1–6, 2018. doi:10.1038/s41467-018-07090-4.
- [26] Roberto Oliveira and Barbara M Terhal. The complexity of quantum spin systems on a two-dimensional square lattice. *arXiv:quant-ph/0504050*, 2005. URL: <https://arxiv.org/abs/quant-ph/0504050>.
- [27] Alberto Peruzzo, Jarrod McClean, Peter Shadbolt, Man-Hong Yung, Xiao-Qi Zhou, Peter J. Love, Alán Aspuru-

- Guzik, and O'Brien Jeremy L. A variational eigenvalue solver on a photonic quantum processor. *Nature Communications*, 5(1):4213, 2014. URL: <https://doi.org/10.22331/10.1038/ncomms5213>, doi:10.1038/ncomms5213.
- [28] David Poulin, Alexei Kitaev, Damian S. Steiger, Matthew B. Hastings, and Matthias Troyer. Quantum Algorithm for Spectral Measurement with a Lower Gate Count. *Physical review letters*, 121:010501, Jul 2018. URL: <https://link.aps.org/doi/10.1103/PhysRevLett.121.010501>, doi:10.1103/PhysRevLett.121.010501.
- [29] Jérémie Roland and Nicolas J. Cerf. Quantum Search by Local Adiabatic Evolution. *Physical Review A*, 65:042308, Mar 2002. URL: <https://link.aps.org/doi/10.1103/PhysRevA.65.042308>, doi:10.1103/PhysRevA.65.042308.
- [30] Christof Zalka. Grover's quantum searching algorithm is optimal. *Physical Review A*, 60:2746–2751, Oct 1999. URL: <https://link.aps.org/doi/10.1103/PhysRevA.60.2746>, doi:10.1103/PhysRevA.60.2746.